

**Characterizing the structural and folding properties of long-sequence
hypomurocin B peptides and their analogs**

János Horváth,¹ Zoltán Násztor,¹ Ferenc Bartha,² Ferenc Bogár,³ Balázs Leitgeb^{1,4}

¹Institute of Biophysics, Biological Research Centre, Hungarian Academy of Sciences,
Temesvári krt. 62, H-6726 Szeged, Hungary

²Department of Medical Chemistry, Faculty of Medicine, University of Szeged,
Dóm tér 8, H-6720 Szeged, Hungary

³MTA-SZTE Supramolecular and Nanostructured Materials Research Group of Hungarian
Academy of Sciences, University of Szeged, Dóm tér 8, H-6720 Szeged, Hungary

⁴Department of Microbiology, Faculty of Science and Informatics, University of Szeged,
Közép fasor 52, H-6726 Szeged, Hungary

Corresponding author:

Dr. Balázs Leitgeb

Institute of Biophysics,

Biological Research Centre,

Hungarian Academy of Sciences,

Temesvári krt. 62, H-6726 Szeged, Hungary

Tel.: +36-62-599-726

Fax: +36-62-433-133

e-mail: leitgeb.balazs@brc.mta.hu

This article has been accepted for publication and undergone full peer review but has not been through the copyediting, typesetting, pagination and proofreading process which may lead to differences between this version and the Version of Record. Please cite this article as an 'Accepted Article', doi: 10.1002/bip.00000

ABSTRACT

We studied the folding processes of long-sequence hypomurocin peptides and their analogs by means of molecular dynamics methods, focusing on the formation of various helical structures and intramolecular H-bonds. The evolution of different helical conformations, such as the 3_{10} -, α - and left-handed α -helices, was examined, taking into account the entire sequence and each amino acid of peptides. The results indicated that the hypomurocin peptides and their analogs possessed a propensity to adopt helical conformations, and they showed a preference for the 3_{10} -helical structure over the α -helical one. The evolution of a variety of the intramolecular H-bonds, including local and non-local interactions, was also investigated. The results pointed out that on the one hand, the appearance of local, helix-stabilizing H-bonds correlated with the presence of helical conformations, and on the other hand, the non-local H-bonds did not affect significantly the formation of helical structures. Additionally, comparing the structural and folding features of hypomurocin peptides and their analogs, our study led to the observation that the L-D isomerism of isovaline amino acid induced effects on the folding processes of these long-sequence peptaibol molecules. Accordingly, the hypomurocin peptides and their analogs could be characterized by typical structural and folding properties.

Keywords: hypomurocin; peptaibol; molecular dynamics; helical structure; intramolecular H-bond

INTRODUCTION

Hypomurocins are fungal peptides belonging to the peptaibol family,¹⁻³ which show antibiotic and hemolytic activities, and they were isolated from the fungus *Hypocrea muroiana*.⁴ According to their sequence length, two different groups of hypomurocin (HM) molecules could be distinguished, such as the short-sequence HM A peptides, as well as the long-sequence HM B peptides.⁴ The former group of hypomurocins includes six peptides consisting of 11 amino acid residues, while the latter one comprises also six peptides composed of 18 amino acids. The HM molecules contain non-proteinogenic amino acids (*i.e.* α -aminoisobutyric acid, Aib; and isovaline, Iva), and their N-terminal residue is acetylated, and furthermore, an amino alcohol (*i.e.* leucinol, Leuol; and valinol, Valol) is linked at their C-terminal end.

The three-dimensional structure of short-sequence HM A peptides was previously investigated by both experimental and theoretical methods. For the HM A-1, HM A-3 and HM A-5 molecules, the NMR measurements led to the observation that these peptides adopted a mixed helical conformation, containing not only α - and 3_{10} -helices, but also type I β -turn structure.^{5,6} In the case of all six HM A peptides, the results derived from our earlier theoretical study indicated that these short-sequence peptaibol molecules could be characterized by β -turn structures or 3_{10} -helical conformation rather than by α -helical structure.⁷ In contrast to the case of HM A peptides, the three-dimensional structure of long-sequence HM B peptides has not been examined, so far.

In this theoretical study, the folding processes of six HM B molecules (see Table I) were explored in detail, in order to determine their typical structural and folding features. As the amino acid sequences represented in Table I indicated, among the HM B peptides, three molecules (*i.e.* HM B-3b, HM B-4 and HM B-5) possess the D-isomer of Iva residue. To

investigate the effects of the L-D isomerism of Iva amino acid on the folding processes of these long-sequence HM B peptides, the structural and folding properties of the L-Iva-containing analogs of above-mentioned three molecules were also studied. In the case of these analogs, the D-Iva residue was substituted by L-Iva amino acid (see Table I), which is located **at position 7 of the HM B-3b peptide** (*i.e.* [L-Iva⁷]HM B-3b), as well as **at position 11 of the HM B-4 and HM B-5 peptides** (*i.e.* [L-Iva¹¹]HM B-4 and [L-Iva¹¹]HM B-5).

METHODS

Since the HM B peptides and their analogs contain non-proteinogenic amino acids (*i.e.* Aib, D-Iva and L-Iva), as well as amino alcohol residues (*i.e.* Leuol and Valol), these non-standard residues were parameterized by means of quantum chemical calculations. In the course of parameterization procedure, the second-order Møller-Plesset perturbation method and the 6-311G basis set were used. To calculate the partial atomic charges for the non-proteinogenic amino acids and amino alcohol residues, the restrained electrostatic potential (RESP) method was applied.

For the HM B peptides and their analogs, molecular dynamics (MD) calculations were performed, in order to study and identify the structural and folding features of these long-sequence peptaibol molecules. The MD simulations were carried out with the AMBER 9 software,⁸ for which the AMBER 99SB force field⁹ and the Generalized Born implicit solvent model¹⁰⁻¹² were applied. The MD calculations were performed at 300 K, using the Langevin model to regulate the temperature during the simulations. The time step was set to 2 fs, and each bond including hydrogen atom was constrained by the SHAKE algorithm applying a tolerance of 10^{-4} Å. Furthermore, no cutoff was used in the case of non-bonding interactions. For each HM B peptide, the MD calculations were started from the same conformation

derived from an initial energy-minimization. Afterwards, 100 individual 100-ns-long MD simulations with random starting velocities were carried out in the case of all HM B molecules, and the MD trajectories were sampled in every ps.

RESULTS AND DISCUSSION

Helicities for Whole Conformation

For the HM B peptides and their analogs, the evolution of different helical structures was examined, as follows: *i*) 3_{10} -helix, *ii*) α -helix and *iii*) left-handed α -helix. In the case of each conformation of peptides, with regard to each snapshot of the MD trajectories, the following formula was used to calculate the percentages of various helical contents (*i.e.* helicities, *f*):¹³⁻¹⁵

$$f = \frac{n_h}{N} \cdot 100 \quad (1)$$

where n_h is the number of amino acid residues satisfying the torsion angle criteria for the various helical conformations, which were as follows: *i*) $\Phi = -60^\circ \pm 30^\circ$ and $\Psi = -30^\circ \pm 30^\circ$ for the 3_{10} -helix,¹⁶ *ii*) $\Phi = -60^\circ \pm 30^\circ$ and $\Psi = -50^\circ \pm 30^\circ$ for the α -helix¹⁶ and *iii*) $\Phi = 60^\circ \pm 30^\circ$ and $\Psi = 50^\circ \pm 30^\circ$ for the left-handed α -helix.¹⁵ The N is the number of all amino acid residues found in the sequences of peptides, namely, $N = 18$ for the HM B peptides and their analogs.

To characterize the helix-forming propensities of peptides, average helicities (f_{AVE-S}) were calculated for the ensemble of 100 individual MD calculations, as follows:¹³⁻¹⁵

$$f_{AVE} = \frac{\sum_{i=1}^M \frac{n_{hi}}{N}}{M} \cdot 100 \quad (2)$$

where n_{hi} is the number of amino acid residues located in certain helical region for the i th MD trajectory, N is the same as for the previous formula, such as $N = 18$, and M is the number of individual MD simulations, such as $M = 100$. The f_{AVE} values were calculated for the 3_{10} -, α - and left-handed α -helices, respectively, and they were labeled as $f_{AVE}(3_{10})$, $f_{AVE}(\alpha)$ and $f_{AVE}(L\alpha)$, respectively.

The alterations of various average helicities as a function of simulation time in the case of HM B peptides and their analogs are shown in Figure 1. Based on the f_{AVE} vs. time plots, it could be concluded that the average helicities increased first monotonically, and then they fluctuated around their maximum values, taking into account each type of the helical contents. As the helicity curves indicated, different final values of f_{AVE} were detected by the end of MD simulations, with regard to the various helical contents (see Table II). The helicity curves represented in Figure 1, and the values of average helicities shown in Table II pointed out that for all peptides, the values of $f_{AVE}(3_{10})$ proved to be larger as compared to those of $f_{AVE}(\alpha)$, and nevertheless, the values of $f_{AVE}(L\alpha)$ were the lowest. These observations revealed that the HM B peptides and their analogs could be characterized by 3_{10} -helical structure rather than by α -helical conformation.

Based on the average helicities vs. time plots, considering the nature of helicity curves, two different groups of HM B molecules could be distinguished. For the first group, including the HM B-1, HM B-2 and HM B-3a peptides, as well as the three L-Iva-containing analogs (*i.e.* [L-Iva⁷]HM B-3b, [L-Iva¹¹]HM B-4 and [L-Iva¹¹]HM B-5), the helicity curves showed similar characteristics, taking into account the 3_{10} -, α - and left-handed α -helical contents, respectively (see Figure 1). For the second group, covering the three HM B peptides possessing D-Iva amino acid (*i.e.* HM B-3b, HM B-4 and HM B-5), the helicity curves were found to be also similar, regarding the 3_{10} -, α - and left-handed α -helical contents, respectively (see Figure 1). However, comparing the above-mentioned two groups of

peptides, the various types of helicity curves showed different characteristics (see Figure 1). As the average helicities vs. time plots indicated, the initial slopes of curves were found to be larger for the former group of molecules, in comparison with those observed in the case of the latter group of molecules. These observations revealed that the HM B-1, HM B-2 and HM B-3a peptides, as well as the three L-Iva-containing analogs reached their final values of f_{AVE} s sooner than the HM B-3b, HM B-4 and HM B-5 peptides. On the basis of data shown in Table II, it could be concluded that for the former molecules, the values of $f_{AVE}(3_{10})$ were slightly larger, while the values of $f_{AVE}(\alpha)$ and $f_{AVE}(L\alpha)$ were slightly lower, as compared to those detected in the case of latter molecules.

Helicities for Amino Acid Residues

The 3_{10} -, α - and left-handed α -helical contents averaged over the 100 individual MD trajectories were calculated not only for the whole conformation, but also for each amino acid residue of the HM B peptides and their analogs. The alterations of different average helicities per residue as a function of simulation time were illustrated in contour plots (see Figures 2-4), which type of representation was earlier used for Lys- and Arg-containing Ala-based peptides,^{13,14} as well as for long-sequence trichobrachin molecules.¹⁵

Based on the contour plots with regard to the 3_{10} - and α -helical contents (see Figures 2 and 3), it could be concluded that the structure of HM B peptides and their analogs can be characterized by two helical segments located in the N- and C-terminal parts of molecules, respectively. Among them, the N-terminal helical part was found to be longer than the C-terminal helical part in the case of each HM B peptide (see Figures 2 and 3). The contour plots also indicated that the two helical segments were separated by a region possessing lower propensity to adopt 3_{10} - or α -helical conformation, which was located near the Pro¹³ amino

acid (see Figures 2 and 3). On the basis of above-mentioned results, it could be proposed that the long-sequence HM B peptides showed a tendency to fold into two shorter, separated helices rather than a longer, continuous one. **Based on the crystal structure of alamethicin,¹⁷ a similar secondary structural motif was observed for this most extensively studied, long-sequence peptaibol composed of 20 amino acids.^{18,19} These results pointed out that alamethicin could be characterized by mainly α -helical structure, which possessed a small distortion generated by the Pro¹⁴ amino acid. Consequently, this peptaibol molecule adopted a conformation, for which the two helical segments found in the N- and C-terminal parts of alamethicin, respectively, were linked by a bend structure near the Pro residue located at position 14. Similarly to the case of alamethicin, this secondary structural motif was also observed in the case of other long-sequence peptaibol molecules.¹**

Taking into account the contour plots concerning the left-handed α -helical contents (see Figure 4), it could be seen that this helical conformation could be detected in the case of Aib and Gly amino acids of each HM B molecule, as well as in the case of the D-Iva residues of HM B-3b, HM B-4 and HM B-5 peptides. **As it was described earlier, the Aib amino acid as an achiral residue could adopt both the right-handed and left-handed helical conformations.²⁰ The analysis of contour plots led to the observation that certain achiral amino acids, as well as the D-amino acid residues could be characterized by a larger propensity to adopt the left-handed α -helical structure than the other achiral amino acids of peptides.** These are as follows: *i*) for the HM B-1 molecule: the Aib⁷, Aib⁹, Gly¹⁰, Aib¹¹, Aib¹², Aib¹⁵ and Aib¹⁶ amino acids; *ii*) in the case of HM B-2 and HM B-3a peptides: the Aib⁵, Aib⁷, Aib⁹, Gly¹⁰, Aib¹¹, Aib¹², Aib¹⁵ and Aib¹⁶ amino acids; *iii*) for the HM B-3b molecule: the Aib⁵, D-Iva⁷, Aib⁹, Gly¹⁰, Aib¹¹, Aib¹⁵ and Aib¹⁶ amino acids; *iv*) in the case of HM B-4 and HM B-5 peptides: the Aib⁵, Aib⁷, Aib⁹, D-Iva¹¹, Aib¹², Aib¹⁵ and Aib¹⁶ amino

acids; *v*) for the [L-Iva⁷]HM B-3b molecule: the Aib⁵, Aib⁹, Gly¹⁰, Aib¹¹, Aib¹², Aib¹⁵ and Aib¹⁶ amino acids; *vi*) in the case of [L-Iva¹¹]HM B-4 and [L-Iva¹¹]HM B-5 peptides: the Aib⁵, Aib⁷, Aib⁹, Gly¹⁰, Aib¹², Aib¹⁵ and Aib¹⁶ amino acids.

Intramolecular H-Bonds for Whole Conformation

For the HM B peptides and their analogs, the evolution of different intramolecular H-bonds formed between the backbone NH donor and CO acceptor groups was investigated. Among them, the group of so-called local H-bonds comprises the following helix-stabilizing interactions: *i*) in the case of 3_{10} -helix, the $i \leftarrow i+3$ (or $l \leftarrow 4$) H-bonds evolved between a NH group of $i+3$ th and a CO group of i th amino acids; *ii*) in the case of α - and left-handed α -helices, the $i \leftarrow i+4$ (or $l \leftarrow 5$) H-bonds formed between a NH group of $i+4$ th and a CO group of i th residues. The other group of intramolecular H-bonds, such as the so-called non-local H-bonds, includes two types of interactions, as follows: *i*) the $i \leftarrow i+n$ H-bonds evolved between the backbone CO and NH groups, where $n > 4$; *ii*) all types of $i \rightarrow i+n$ H-bonds formed between the backbone NH and CO groups. For all the interactions mentioned afore, an intramolecular H-bond was assumed to exist if the $N \cdots O$ distance between the N and O atoms of NH and CO groups was within 3.5 Å, and if the $N-H \cdots O$ angle subtended at the H atom by the bond to the C atom and the line joining the H and O atoms was larger than 120°. In the case of HM B peptides and their analogs, the presence of local and non-local H-bonds was studied along the entire sequence of molecules. Based on the 100 individual MD trajectories, the average numbers of $i \leftarrow i+3$, $i \leftarrow i+4$ and non-local H-bonds were calculated, respectively, and they were labeled as HB₁₋₄, HB₁₋₅ and HB_{NL}, **respectively**.

The alterations of HB₁₋₄ and HB₁₋₅, presented in Figure 5, indicated an increasing tendency first, followed by a fluctuation around a certain value for all HM B peptides and

their analogs. Based on the Figure 5, it could be seen that in the case of HB₁₋₄ and HB₁₋₅ curves, also a saturation-like behavior could be found, as it was earlier observed in the case of helicity curves. Table III represents the final average numbers of $i \leftarrow i+3$ and $i \leftarrow i+4$ H-bonds, which were detected by the end of MD calculations for each HM B molecule. The HB₁₋₄ and HB₁₋₅ curves, as well as the average numbers of local H-bonds pointed out that in the case of HM B peptides and their analogs, the amount of $i \leftarrow i+3$ H-bonds proved to be larger than the amount of $i \leftarrow i+4$ H-bonds. This relationship between the two types of local H-bonds correlates with the observation made previously for the relationship between the $f_{AVE}(3_{10})$ and $f_{AVE}(\alpha)$, namely, the 3_{10} -helical content was found to be larger than the α -helical content in the case of each HM B molecule.

Taking into account the nature of HB₁₋₄ and HB₁₋₅ curves, the HM B molecules could be divided into two different groups. One of them comprises the HM B-1, HM B-2 and HM B-3a peptides, as well as the three L-Iva-containing analogs (*i.e.* [L-Iva⁷]HM B-3b, [L-Iva¹¹]HM B-4 and [L-Iva¹¹]HM B-5), while the other group includes the three HM B peptides possessing D-Iva amino acid (*i.e.* HM B-3b, HM B-4 and HM B-5). Based on Figure 5, it could be concluded that the HB₁₋₄ and HB₁₋₅ curves could be characterized by a similar nature for the former group of molecules, as well as for the latter group of molecules, respectively. Nevertheless, the HB₁₋₄ and HB₁₋₅ curves showed different characteristics, concerning the above-mentioned two groups of HM B molecules (see Figure 5). Accordingly, the HB₁₋₄ and HB₁₋₅ reached their maximum sooner, as well as the initial slopes of curves were larger for the HM B-1, HM B-2 and HM B-3a peptides, as well as for the three L-Iva-containing analogs, than for the HM B-3b, HM B-4 and HM B-5 peptides (see Figure 5). These observations are in good agreement with the previous findings made in the case of HM B molecules, with regard to the helicity curves, taking into account the 3_{10} - and α -helical contents. On the basis of data presented in Table III, it could be seen that considering the final average numbers of

$i \leftarrow i+3$ H-bonds, significant differences could not be detected between the afore-mentioned two groups of HM B molecules. However, it could be concluded that a larger amount of the $i \leftarrow i+4$ H-bonds could be observed for the three D-Iva-containing HM B peptides, as compared to those found for the HM B-1, HM B-2 and HM B-3a peptides, as well as for the three HM B analogs possessing L-Iva amino acid (see Table III).

The alterations of HB_{NL} as a function of simulation time are shown in Figure 5, while the final average numbers of these types of H-bonds are represented in Table III, in the case of HM B peptides and their analogs. On the basis of HB_{NL} curves, it could be concluded that few non-local H-bonds appeared at an early stage of the MD calculations, however, in the majority of cases, their average numbers decreased subsequently by the end of simulation. As these HB_{NL} curves revealed, the average numbers of non-local H-bonds decreased as a function of simulation time, whereas an increasing tendency could be simultaneously detected, concerning the $i \leftarrow i+3$ and $i \leftarrow i+4$ H-bonds. Among the HM B molecules, for the HM B-4 and HM B-5 peptides containing D-Iva amino acid **at position 11**, different characteristics could be observed, namely, the average numbers of non-local H-bonds did not show a decreasing tendency during the MD simulations, but they fluctuated around a certain value. Based on the HB_{NL} curves (see Figure 5), as well as on data shown in Table III, it could be seen that the final average numbers of non-local H-bonds were found to be the lowest by the end of simulations, in comparison with those observed for the $i \leftarrow i+3$ and $i \leftarrow i+4$ H-bonds.

As it was mentioned previously, on the basis of helicity curves concerning the 3_{10} - and α -helices, as well as of HB_{1-4} and HB_{1-5} curves, two distinct groups of HM B molecules could be distinguished. Considering the non-local H-bonds, differences could be also detected between the two groups of HM B molecules. As the HB_{NL} curves represented in Figure 5, as well as data displayed in Table III pointed out, taking into account the whole simulation time, the non-local H-bonds appeared with lower frequency for the HM B-1, HM B-2 and HM B-3a

peptides, as well as for the three L-Iva-containing analogs, than in the case of three HM B peptides possessing D-Iva amino acid. Based on these results, it could be suggested that the non-local H-bonds could presumably produce effects on the formation of helical structures, as well as on the folding processes for the latter group of HM B molecules, while these intramolecular interactions seemed to not affect the evolution of helical conformations for the former group of HM B molecules.

Intramolecular H-Bonds for Amino Acid Residues

As for the average helicities mentioned previously, the alterations of $i \leftarrow i+3$ and $i \leftarrow i+4$ H-bonds were examined not only for the whole conformation of HM B molecules, but also for all amino acids of peptides. To characterize the H-bond-forming propensities of each amino acid residue as an H-bond donor, contour plots were produced in the case of HM B peptides and their analogs (see Figures 6 and 7), for which the alterations of average $i \leftarrow i+3$ and $i \leftarrow i+4$ H-bonds per residue were represented as a function of simulation time.

The analysis of contour plots regarding the $i \leftarrow i+3$ H-bonds led to the similar observation, as it was made earlier in the case of contour plots concerning the 3_{10} -helical content. Consequently, for all HM B molecules, two regions displaying larger propensity to form $i \leftarrow i+3$ H-bonds could be observed, which were located at the N- and C-terminal parts of peptides, respectively (see Figure 6). As the contour plots revealed, these two regions were separated by the Pro¹³ amino acid (see Figure 6), which could not form intramolecular H-bonds as a donor residue. These results also suggested that the structure of long-sequence HM B peptides could be characterized by two shorter helices rather than a longer, continuous helical conformation. The contour plots with regard to the $i \leftarrow i+3$ H-bonds indicated that several amino acids showed larger propensity to form $i \leftarrow i+3$ H-bonds as a donor residue, as

compared to other amino acids of HM B peptides (see Figure 6). They were as follows: *i*) for the HM B-1, HM B-2 and HM B-3a molecules: the Leu⁴, Aib⁷, Aib⁹, Gly¹⁰, Aib¹¹, Leu¹⁴ and Gln¹⁷ amino acids; *ii*) in the case of HM B-3b peptide: the Leu⁴, Aib¹¹, Leu¹⁴ and Gln¹⁷ amino acids; *iii*) for the HM B-4 and HM B-5 molecules: the Leu⁴, Aib⁷, Aib⁹, Leu¹⁴ and Gln¹⁷ amino acids; *iv*) in the case of [L-Iva⁷]HM B-3b and [L-Iva¹¹]HM B-4 peptides: the Leu⁴, L-Iva⁷/Aib⁷, Aib⁹, Gly¹⁰, Leu¹⁴ and Gln¹⁷ amino acids; *v*) for the [L-Iva¹¹]HM B-5 molecule: the Leu⁴, Aib⁷, Gly¹⁰, Leu¹⁴ and Gln¹⁷ amino acids.

Considering the contour plots with regard to the $i \leftarrow i+4$ H-bonds, few residues could be also detected for all HM B molecules, which possessed larger propensity to participate in the $i \leftarrow i+4$ H-bonds as a donor, in comparison with other amino acids of peptides (see Figure 7).

Accordingly, the following residues could be characterized by larger H-bond-forming propensity: *i*) for the HM B-1, HM B-2, HM B-3a, [L-Iva¹¹]HM B-4 and [L-Iva¹¹]HM B-5 molecules: the Aib⁵, Aib⁷, Gly¹⁰ and Leu¹⁸/Val¹⁸ residues; *ii*) in the case of HM B-3b peptide: the Aib⁵, D-Iva⁷, Val⁸, Gly¹⁰, Aib¹⁵ and Val¹⁸ residues; *iii*) for the HM B-4 and HM B-5 molecules: the Aib⁵, Aib⁷, Aib⁹, Gly¹⁰, Aib¹⁵ and Leu¹⁸/Val¹⁸ residues; *iv*) in the case of [L-Iva⁷]HM B-3b peptide: the Aib⁵, Gly¹⁰ and Val¹⁸ residues.

To further characterize the $i \leftarrow i+3$ and $i \leftarrow i+4$ H-bonds evolved along the entire sequence of molecules, another type of graphical representation was applied (see Figures 8 and 9). In this case, the presence or absence of various $i \leftarrow i+3$ and $i \leftarrow i+4$ H-bonds were represented, as well as the values of final average H-bonds, detected by the end of MD simulations, were demonstrated throughout the peptide sequences. For both types of H-bonds, the whole range regarding the values of final average H-bonds was divided into four equal regions. According to the values of final average H-bonds belonging to the different regions, the evolving $i \leftarrow i+3$ and $i \leftarrow i+4$ H-bonds were illustrated by bars with distinct thicknesses (*i.e.* for lower value, thinner bar; as well as

for higher value, thicker bar was used), which connected the residues participating in the formation of intramolecular H-bonds. For the absence of $i \leftarrow i+3$ and $i \leftarrow i+4$ H-bonds, a bar was not represented with regard to the two residues. Based on these plots, similar observations could be made as for the earlier results, furthermore, differences could be also observed between the two groups of HM B molecules mentioned previously, taking into account the H-bonding patterns represented in Figures 8 and 9.

CONCLUSIONS

In this study, the evolution of helical structures and intramolecular H-bonds was examined for the long-sequence HM B peptides and their analogs. The formation of various helical structures was investigated with regard to the entire sequence of molecules, as well as to each amino acid of peptides. The results revealed that the HM B peptides and their analogs showed a propensity to adopt helical conformations, and nevertheless, these long-sequence peptaibol molecules could be characterized by 3_{10} -helical structure rather than by α -helical structure. The formation and role of different intramolecular H-bonds, including local and non-local interactions, were also studied for the HM B peptides and their analogs. The presence of $i \leftarrow i+3$ and $i \leftarrow i+4$ H-bonds correlated with the appearance of helical conformations, indicating the relevant helix-stabilizing role of these intramolecular H-bonds. On the basis of results concerning the non-local H-bonds, it could be concluded that these interactions did not produce significant effects on the formation of helical structures, as well as on the folding processes of HM B molecules. In our theoretical study, it was also examined how the L-D isomerism of Iva amino acid affected the structural and folding properties of long-sequence HM B peptides. Taking into account the evolution of helical structures and intramolecular H-bonds, the analysis of results led to the following observations. On the one

hand, the L-Iva-containing analogs showed different characteristics as compared to the HM B molecules possessing D-Iva residue, and on the other hand, the three analogs could be characterized by a similar behavior as observed for the HM B molecules without Iva residue. Accordingly, it could be suggested that the L-D isomerism of Iva amino acid could produce effects on the folding processes of long-sequence HM B peptides. In summary, a comprehensive characterization of the structural properties of HM B peptides and their analogs was carried out, and their typical folding features were identified.

ACKNOWLEDGEMENTS

For Balázs Leitgeb, this research was supported by the European Union and the State of Hungary, co-financed by the European Social Fund in the framework of TÁMOP-4.2.4.A/2-11/1-2012-0001 „National Excellence Program – Elaborating and operating an inland student and researcher personal support system convergence program”. This research was supported by the Hungarian Scientific Research Fund (OTKA K 106000).

REFERENCES

1. Szekeres, A.; Leitgeb, B.; Kredics, L.; Antal, Z.; Hatvani, L.; Manczinger, L.; Vágvölgyi, C. *Acta Microbiol Immunol Hung* 2005, 52, 137–168.
2. Peptaibiotics, *Chem Biodivers* 2007, 4, 1021–1412.
3. Peptaibiotics II, *Chem Biodivers* 2013, 10, 731–961.
4. Becker, D.; Kiess, M.; Brückner, H. *Liebigs Ann/Recueil* 1997, 4, 767–772.
5. Pradeille, N.; Zerbe, O.; Möhle, K.; Linden, A.; Heimgartner, H. *Chem Biodivers* 2005, 2, 1127–1152.

6. Pradeille, N.; Tzouros, M.; Möhle, K.; Linden, A.; Heimgartner, H. *Chem Biodivers* 2012, 9, 2528–2558.
7. Násztor, Z.; Horváth, J.; Leitgeb, B. *Int J Pept* 2015, Paper 281065.
8. Case, D. A.; Darden, T. A.; Cheatham III, T. E.; Simmerling, C. L.; Wang, J.; Duke, R. E.; Luo, R.; Merz, K. M.; Pearlman, D. A.; Crowley, M.; Walker, R. C.; Zhang, W.; Wang, B.; Hayik, S.; Roitberg, A.; Seabra, G.; Wong, K. F.; Paesani, F.; Wu, X.; Brozell, S.; Tsui, V.; Gohlke, H.; Yang, L.; Tan, C.; Mongan, J.; Hornak, V.; Cui, G.; Beroza, P.; Mathews, D. H.; Schafmeister, C.; Ross, W. S.; Kollman, P. A. *AMBER 9*, University of California, San Francisco, 2006.
9. Hornak, V.; Abel, R.; Okur, A.; Strockbine, B.; Roitberg, A.; Simmerling, C. *Proteins* 2006, 65, 712–725.
10. Hawkins, G. D.; Cramer, C. J.; Truhlar, D. G. *Chem Phys Lett* 1995, 246, 122–129.
11. Hawkins, G. D.; Cramer, C. J.; Truhlar, D. G. *J Phys Chem* 1996, 100, 19824–19839.
12. Tsui, V.; Case, D. A. *Biopolymers (Nucl Acid Sci)* 2000, 56, 275–291.
13. Janzsó, G.; Bogár, F.; Hudoba, L.; Penke, B.; Rákhely, G.; Leitgeb, B. *Comput Biol Chem* 2011, 35, 240–250.
14. Leitgeb, B.; Janzsó, G.; Hudoba, L.; Penke, B.; Rákhely, G.; Bogár, F. *Struct Chem* 2011, 22, 1287–1295.
15. Násztor, Z.; Horváth, J.; Leitgeb, B. *Chem Biodivers* 2015, 12, 1365–1377.
16. Leitgeb, B.; Kerényi, A.; Bogár, F.; Paragi, G.; Penke, B.; Rákhely, G. *J Mol Model* 2007, 13, 1141–1150.
17. **Fox, R. O.; Richards, F. M. *Nature* 1982, 300, 325–330.**
18. **Leitgeb, B.; Szekeres, A.; Manczinger, L.; Vágvölgyi, C.; Kredics, L. *Chem Biodivers* 2007, 4, 1027–1051.**

19. Kredics, L.; Szekeres, A.; Czifra, D.; Vágvölgyi, C.; Leitgeb, B. *Chem Biodivers* 2013, 10, 744–771.

20. Aravinda, S.; Shamala, N.; Balaram, P. *Chem Biodivers* 2008, 5, 1238–1262.

Accepted Article

Table I Amino Acid Sequences of the HM B Peptides and Their Analogs. For the Sequences, Ac is the Acetyl, Aib is the α -Aminoisobutyric Acid, D-Iva is the D-Isovaline, L-Iva is the L-Isovaline, Valol is the Valinol and Leuol is the Leucinol

Peptides	Amino acid sequences
HM B-1	Ac-Aib ¹ -Ser ² -Ala ³ -Leu ⁴ -Aib ⁵ -Gln ⁶ -Aib ⁷ -Val ⁸ -Aib ⁹ -Gly ¹⁰ -Aib ¹¹ -Aib ¹² -Pro ¹³ -Leu ¹⁴ -Aib ¹⁵ -Aib ¹⁶ -Gln ¹⁷ -Valol ¹⁸
HM B-2	Ac-Aib ¹ -Ser ² -Ala ³ -Leu ⁴ -Aib ⁵ -Gln ⁶ -Aib ⁷ -Val ⁸ -Aib ⁹ -Gly ¹⁰ -Aib ¹¹ -Aib ¹² -Pro ¹³ -Leu ¹⁴ -Aib ¹⁵ -Aib ¹⁶ -Gln ¹⁷ -Leuol ¹⁸
HM B-3a	Ac-Aib ¹ -Ala ² -Ala ³ -Leu ⁴ -Aib ⁵ -Gln ⁶ -Aib ⁷ -Val ⁸ -Aib ⁹ -Gly ¹⁰ -Aib ¹¹ -Aib ¹² -Pro ¹³ -Leu ¹⁴ -Aib ¹⁵ -Aib ¹⁶ -Gln ¹⁷ -Valol ¹⁸
HM B-3b	Ac-Aib ¹ -Ser ² -Ala ³ -Leu ⁴ -Aib ⁵ -Gln ⁶ -D-Iva ⁷ -Val ⁸ -Aib ⁹ -Gly ¹⁰ -Aib ¹¹ -Aib ¹² -Pro ¹³ -Leu ¹⁴ -Aib ¹⁵ -Aib ¹⁶ -Gln ¹⁷ -Valol ¹⁸
HM B-4	Ac-Aib ¹ -Ser ² -Ala ³ -Leu ⁴ -Aib ⁵ -Gln ⁶ -Aib ⁷ -Val ⁸ -Aib ⁹ -Gly ¹⁰ -D-Iva ¹¹ -Aib ¹² -Pro ¹³ -Leu ¹⁴ -Aib ¹⁵ -Aib ¹⁶ -Gln ¹⁷ -Valol ¹⁸
HM B-5	Ac-Aib ¹ -Ser ² -Ala ³ -Leu ⁴ -Aib ⁵ -Gln ⁶ -Aib ⁷ -Val ⁸ -Aib ⁹ -Gly ¹⁰ -D-Iva ¹¹ -Aib ¹² -Pro ¹³ -Leu ¹⁴ -Aib ¹⁵ -Aib ¹⁶ -Gln ¹⁷ -Leuol ¹⁸
[L-Iva⁷]HM B-3b	Ac-Aib ¹ -Ser ² -Ala ³ -Leu ⁴ -Aib ⁵ -Gln ⁶ -L-Iva ⁷ -Val ⁸ -Aib ⁹ -Gly ¹⁰ -Aib ¹¹ -Aib ¹² -Pro ¹³ -Leu ¹⁴ -Aib ¹⁵ -Aib ¹⁶ -Gln ¹⁷ -Valol ¹⁸
[L-Iva¹¹]HM B-4	Ac-Aib ¹ -Ser ² -Ala ³ -Leu ⁴ -Aib ⁵ -Gln ⁶ -Aib ⁷ -Val ⁸ -Aib ⁹ -Gly ¹⁰ -L-Iva ¹¹ -Aib ¹² -Pro ¹³ -Leu ¹⁴ -Aib ¹⁵ -Aib ¹⁶ -Gln ¹⁷ -Valol ¹⁸
[L-Iva¹¹]HM B-5	Ac-Aib ¹ -Ser ² -Ala ³ -Leu ⁴ -Aib ⁵ -Gln ⁶ -Aib ⁷ -Val ⁸ -Aib ⁹ -Gly ¹⁰ -L-Iva ¹¹ -Aib ¹² -Pro ¹³ -Leu ¹⁴ -Aib ¹⁵ -Aib ¹⁶ -Gln ¹⁷ -Leuol ¹⁸

Table II Final Average Helicities (in %) Concerning the 3_{10} -, α - and Left-Handed α -Helices for the HM B Peptides and Their Analogs.
 The $f_{AVE}(3_{10})$ Relates to the Average Helicity for the 3_{10} -Helix, the $f_{AVE}(\alpha)$ to the Average Helicity for the α -Helix and the $f_{AVE}(L\alpha)$ to the Average Helicity for the Left-Handed α -Helix

Peptides	Average helicities		
	$f_{AVE}(3_{10})$	$f_{AVE}(\alpha)$	$f_{AVE}(L\alpha)$
HM B-1	55	35	12
HM B-2	57	36	10
HM B-3a	57	36	11
HM B-3b	51	39	17
HM B-4	53	41	16
HM B-5	54	42	15
[L-Iva ⁷]HM B-3b	60	36	10
[L-Iva ¹¹]HM B-4	58	36	10
[L-Iva ¹¹]HM B-5	60	37	9

Table III Final Average Numbers of the Various Types of Intramolecular H-Bonds for the HM B Peptides and Their Analogs. The HB_{1-4} Relates to the Average Number of $i \leftarrow i+3$ H-Bonds, the HB_{1-5} to the Average Number of $i \leftarrow i+4$ H-Bonds and the HB_{NL} to the Average Number of Non-Local H-Bonds

Peptides	Average numbers of H-bonds		
	HB_{1-4}	HB_{1-5}	HB_{NL}
HM B-1	4.09	0.63	0.39
HM B-2	4.02	0.59	0.39
HM B-3a	4.00	0.66	0.35
HM B-3b	4.26	1.06	0.50
HM B-4	4.12	1.02	0.68
HM B-5	4.10	1.07	0.66
[L-Iva ⁷]HM B-3b	4.06	0.51	0.30
[L-Iva ¹¹]HM B-4	3.76	0.68	0.32
[L-Iva ¹¹]HM B-5	3.93	0.59	0.31

FIGURE 1 Alterations of the various average helicities ($f_{\text{AVE-S}}$) as a function of time for (A) HM B-1, (B) HM B-2, (C) HM B-3a, (D) HM B-3b, (E) HM B-4, (F) HM B-5, (G) [L-Iva⁷]HM B-3b, (H) [L-Iva¹¹]HM B-4 and (I) [L-Iva¹¹]HM B-5 peptides. The $f_{\text{AVE}(3_{10})}$ relates to the 3_{10} -helix, the $f_{\text{AVE}(\alpha)}$ to the α -helix and the $f_{\text{AVE}(L\alpha)}$ to the left-handed α -helix.

FIGURE 2 Contour plots concerning the alteration of 3_{10} -helical content per residue as a function of time for (A) HM B-1, (B) HM B-2, (C) HM B-3a, (D) HM B-3b, (E) HM B-4, (F) HM B-5, (G) [L-Iva⁷]HM B-3b, (H) [L-Iva¹¹]HM B-4 and (I) [L-Iva¹¹]HM B-5 peptides.

FIGURE 3 Contour plots concerning the alteration of α -helical content per residue as a function of time for (A) HM B-1, (B) HM B-2, (C) HM B-3a, (D) HM B-3b, (E) HM B-4, (F) HM B-5, (G) [L-Iva⁷]HM B-3b, (H) [L-Iva¹¹]HM B-4 and (I) [L-Iva¹¹]HM B-5 peptides.

FIGURE 4 Contour plots concerning the alteration of left-handed α -helical content per residue as a function of time for (A) HM B-1, (B) HM B-2, (C) HM B-3a, (D) HM B-3b, (E) HM B-4, (F) HM B-5, (G) [L-Iva⁷]HM B-3b, (H) [L-Iva¹¹]HM B-4 and (I) [L-Iva¹¹]HM B-5 peptides.

FIGURE 5 Alterations of the average numbers of the various types of intramolecular H-bonds as a function of time for (A) HM B-1, (B) HM B-2, (C) HM B-3a, (D) HM B-3b, (E) HM B-4, (F) HM B-5, (G) [L-Iva⁷]HM B-3b, (H) [L-Iva¹¹]HM B-4 and (I) [L-Iva¹¹]HM B-5 peptides. The HB_{1-4} relates to the $i \leftarrow i+3$ H-bonds, the HB_{1-5} to the $i \leftarrow i+4$ H-bonds and the HB_{NL} to the non-local H-bonds.

FIGURE 6 Contour plots regarding the alteration of average $i \leftarrow i+3$ H-bonds per residue as a function of time for (A) HM B-1, (B) HM B-2, (C) HM B-3a, (D) HM B-3b, (E) HM B-4, (F) HM B-5, (G) [L-Iva⁷]HM B-3b, (H) [L-Iva¹¹]HM B-4 and (I) [L-Iva¹¹]HM B-5 peptides.

FIGURE 7 Contour plots regarding the alteration of average $i \leftarrow i+4$ H-bonds per residue as a function of time for (A) HM B-1, (B) HM B-2, (C) HM B-3a, (D) HM B-3b, (E) HM B-4, (F) HM B-5, (G) [L-Iva⁷]HM B-3b, (H) [L-Iva¹¹]HM B-4 and (I) [L-Iva¹¹]HM B-5 peptides.

FIGURE 8 Presence or absence of the various $i \leftarrow i+3$ H-bonds, as well as the values of final average H-bonds along the entire sequence for (A) HM B-1, (B) HM B-2, (C) HM B-3a, (D) HM B-3b, (E) HM B-4, (F) HM B-5, (G) [L-Iva⁷]HM B-3b, (H) [L-Iva¹¹]HM B-4 and (I) [L-Iva¹¹]HM B-5 peptides. The thinner bar relates to the lower value, as well as the thicker bar to the higher value of final average H-bonds.

FIGURE 9 Presence or absence of the various $i \leftarrow i+4$ H-bonds, as well as the values of final average H-bonds along the entire sequence for (A) HM B-1, (B) HM B-2, (C) HM B-3a, (D) HM B-3b, (E) HM B-4, (F) HM B-5, (G) [L-Iva⁷]HM B-3b, (H) [L-Iva¹¹]HM B-4 and (I) [L-Iva¹¹]HM B-5 peptides. The thinner bar relates to the lower value, as well as the thicker bar to the higher value of final average H-bonds.

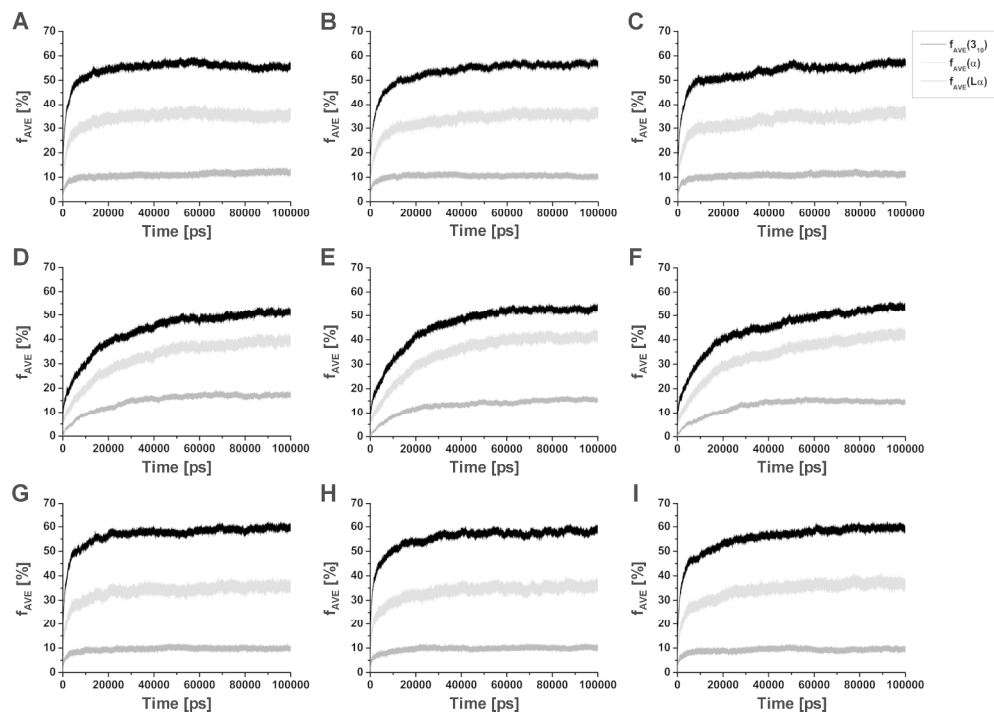


Figure 1

Accepte

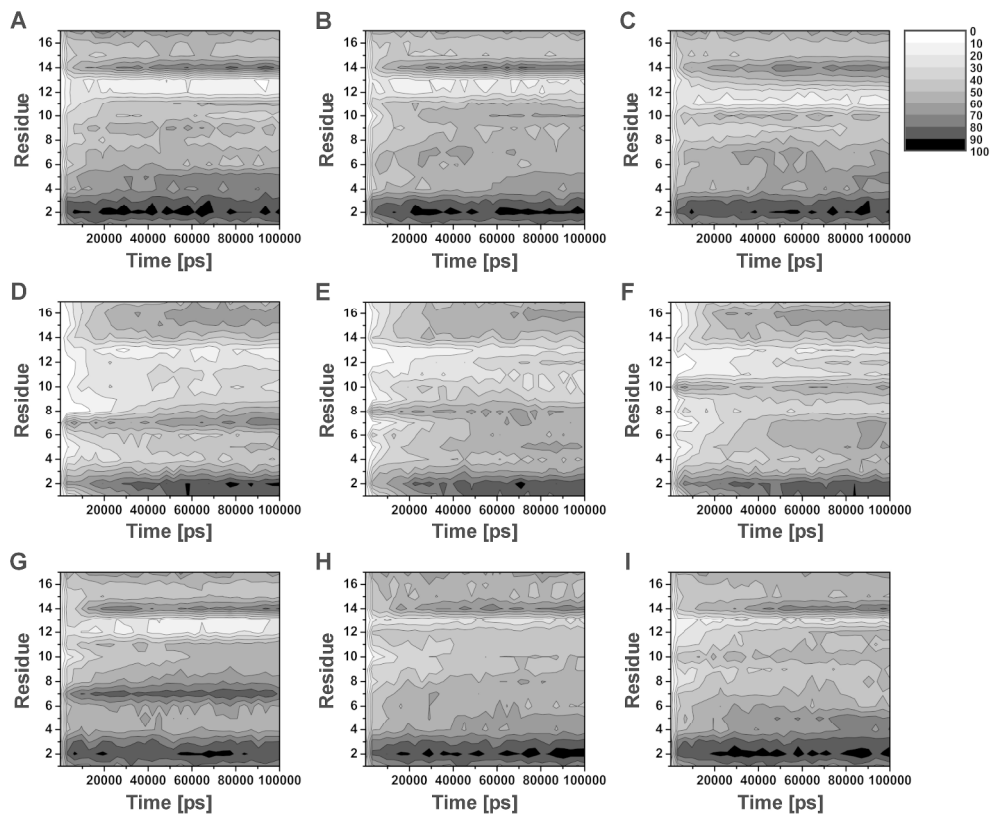


Figure 2

Accept

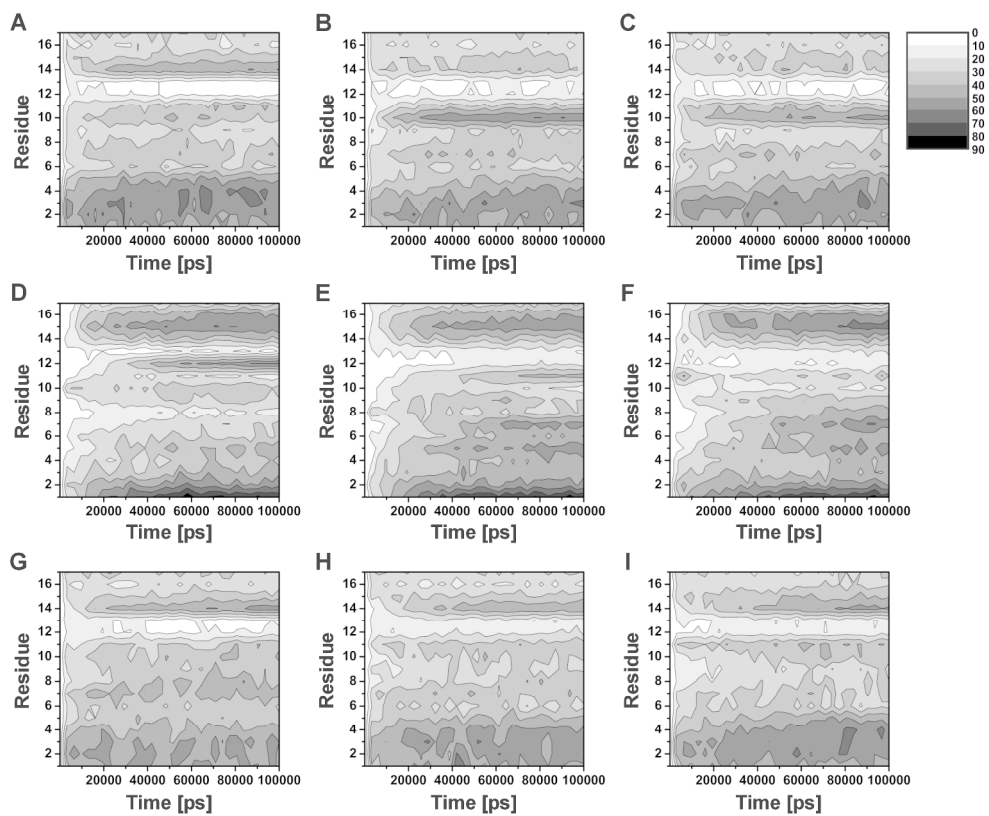


Figure 3

Accept

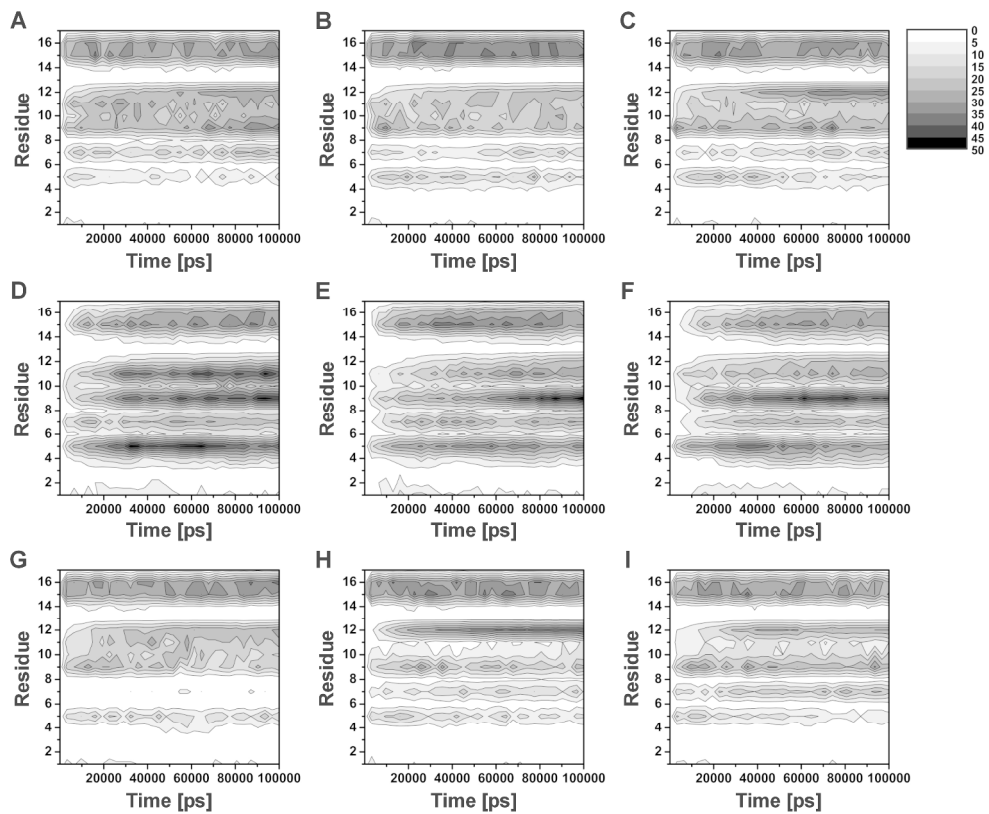


Figure 4

Accept

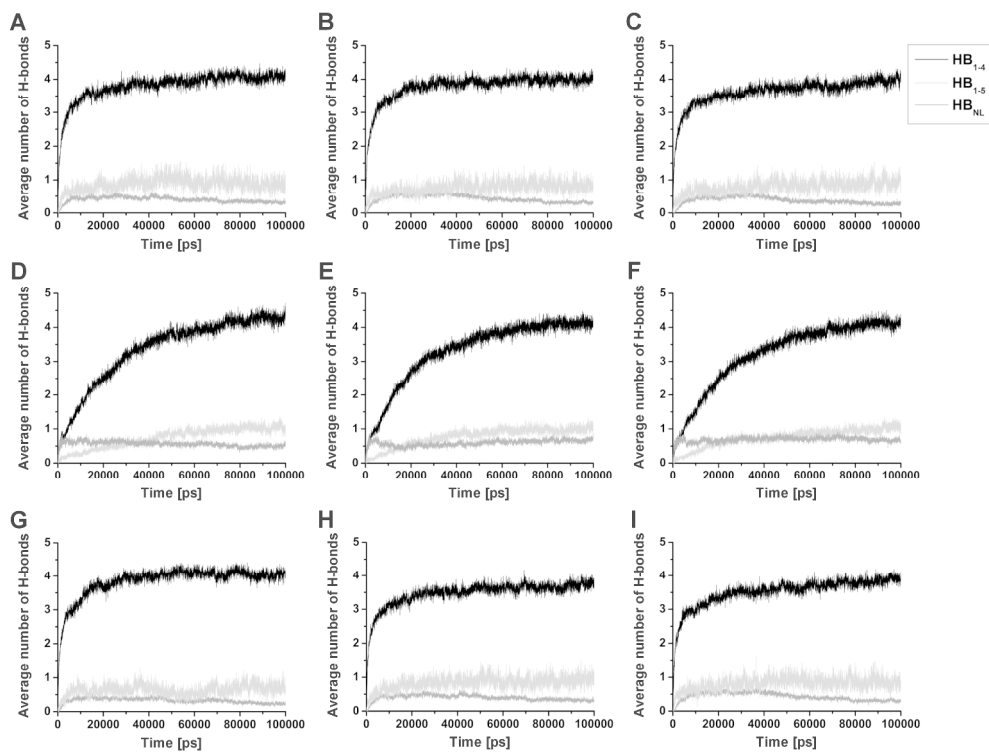


Figure 5

Accept

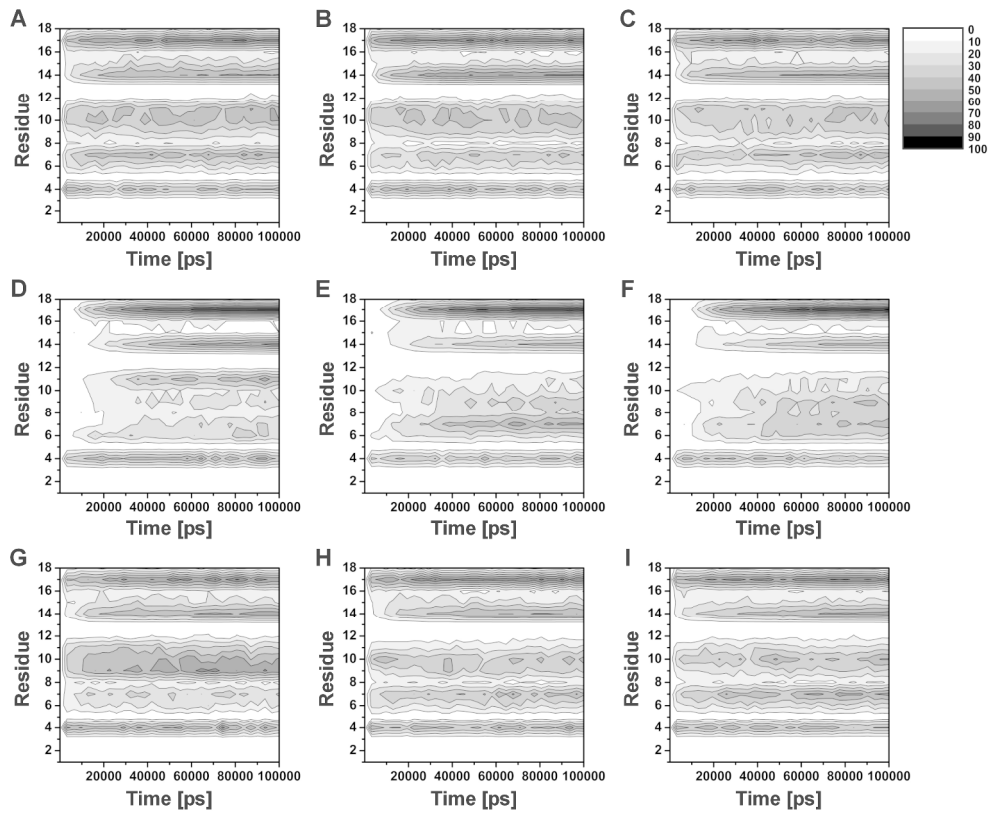


Figure 6

Accept

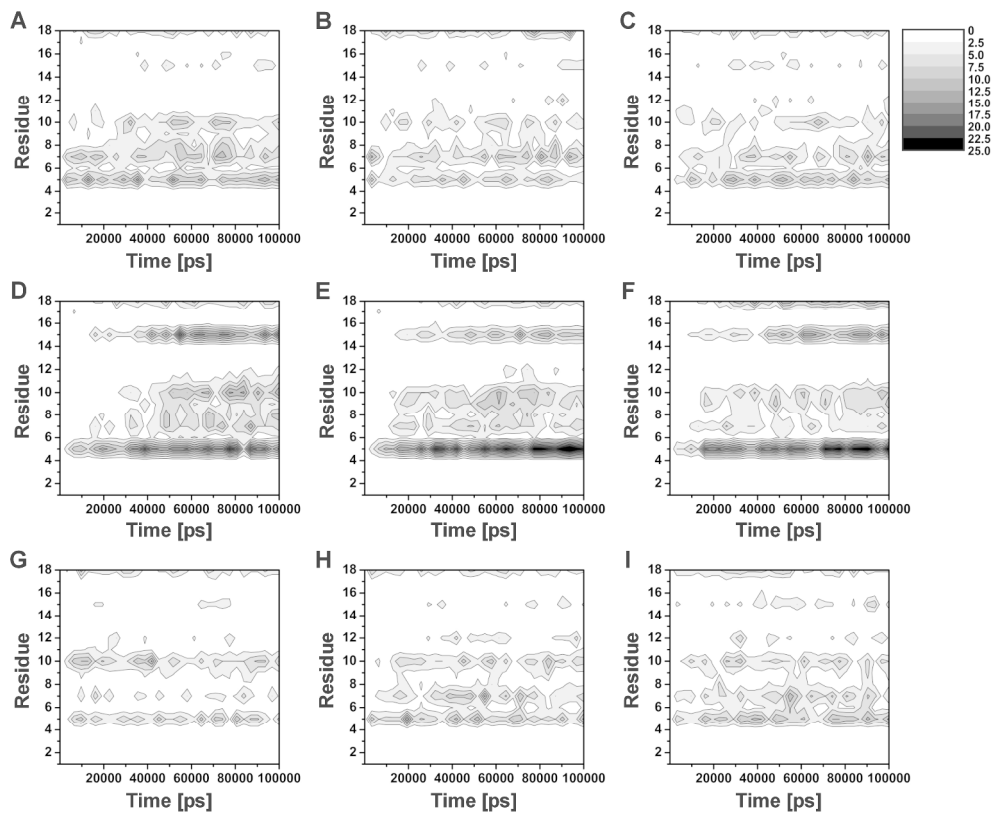


Figure 7

Accept

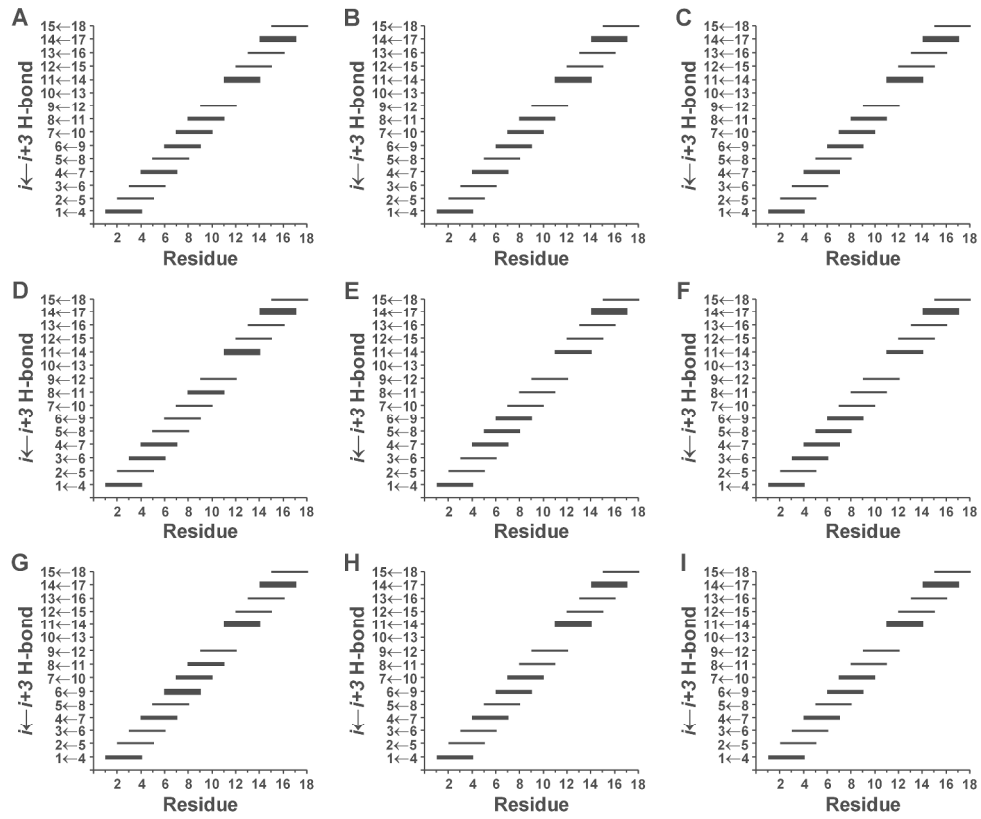


Figure 8

Accep1

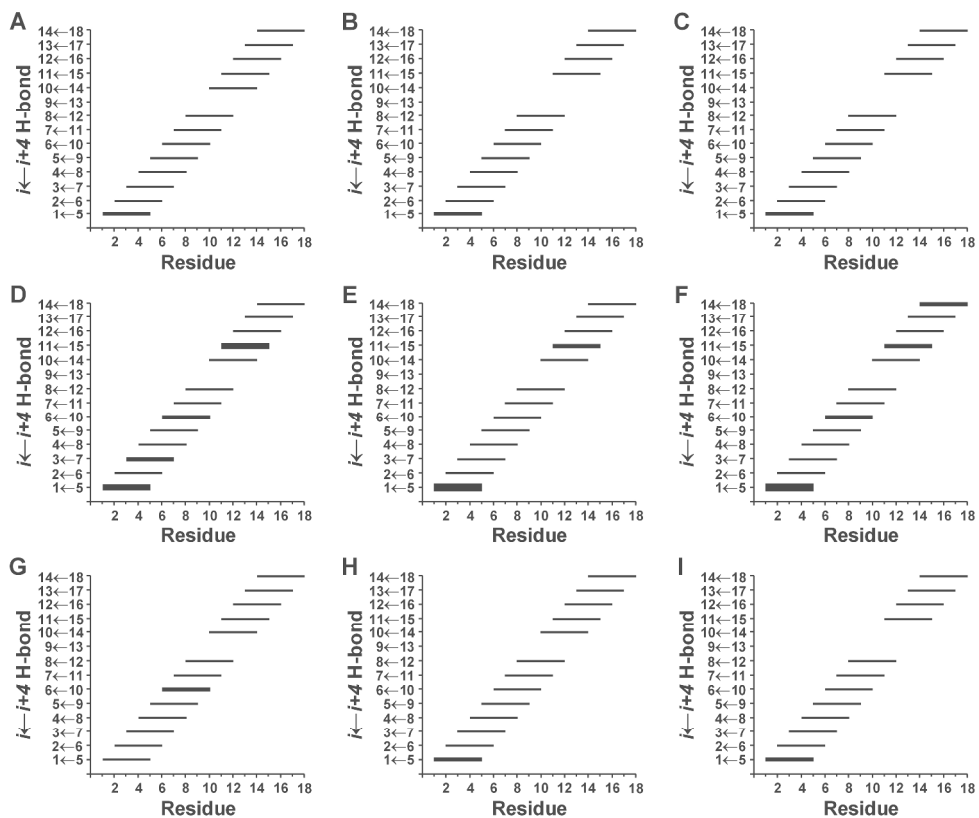


Figure 9

Accep1